

Ultra-distal fine ash occurrences of the Icelandic Askja-S Plinian eruption deposits in Southern Carpathian lakes: new age constraints on a continental scale tephrostratigraphic marker.

Kearney, R.^{a,*}, Albert, P.G.^a, Staff, R.A.^b, Pál, I.^c, Veres, D.^e, Magyari, E.^d, Bronk Ramsey, C.^a

^a Research Laboratory for Archaeology and the History of Art, School of Archaeology, University of Oxford, 1 South Parks Road, Oxford, OX1 3TG, UK.

^b Scottish Universities Environmental Research Centre, University of Glasgow, Rankine Avenue, East Kilbride, South Lanarkshire, G75 0QF, UK.

^c Isotope Climatology and Environmental Research Center (ICER), Institute for Nuclear Research, Hungarian Academy of Sciences, H-4026 Debrecen, Bem tér 18/c, Hungary.

^d Eötvös Lóránd University, MTA-MTM-ELTE Research Group for Paleontology, Department of Environmental and Landscape Geography, Pázmány P. stny. 1/C, H-1117 Budapest, Hungary.

^e Romanian Academy, Institute of Speleology, Clinicilor 5, 400006 Cluj-Napoca, Romania.

*rebecca.kearney@st-annes.ox.ac.uk

Keywords: Askja-S Tephra, Ultra-distal cryptotephra, Carpathian Mountains, Tephrostratigraphy

Highlights

- First cryptotephra investigation from the Southern Carpathian Mountains
- Lakes Brazi and Lia provide the most south-eastern occurrence of the Askja-S tephra
- Furthest south-eastern occurrence of an Icelandic-sourced tephra
- Improved age estimate for the Askja-S eruption of $10,824 \pm 97$ cal years BP
- Highlights potential of additional tephra layers to be found in this region

28

29 **Abstract**

30 Here we present the results of the first cryptotephra investigation of two Late
31 glacial-Holocene lake records from the Southern Carpathian Mountains in Romania, Lake
32 Brazi and Lake Lia. The discovery of an important Icelandic tephrostratigraphic marker, the
33 Askja-S, in the sedimentary records of both sites significantly extends the known ash
34 dispersal from this Plinian eruption. Bayesian age-depth modelling of available radiocarbon
35 (^{14}C) data from both sedimentary records allows us to further refine the depositional age of
36 this ultra-distal tephra. In combination with age constraints on the tephra from other well-
37 dated European sites, we produce an updated age for this key tephrostratigraphic marker of
38 $10,824 \pm 97$ cal yrs BP (95.4% range). The Askja-S tephra is stratigraphically positioned after
39 the palaeoenvironmental proxy response to the Preboreal Oscillation at both sites. The
40 widespread distribution of this tephra across Europe offers the potential to assess spatio-
41 temporal variability of this climatic signal. The discovery of the Askja-S in lake records from
42 the Southern Carpathians highlights the likelihood of finding other ultra-distal (Icelandic)
43 cryptotephra marker layers within the region. Additionally, given the location of the
44 Carpathian region, it offers the opportunity to further enhance and integrate
45 tephrostratigraphic frameworks of north-western Europe with those of the Mediterranean
46 and Anatolia regions, which will enable a more precise comparison of palaeoenvironmental
47 archives across Europe.

48

49

50

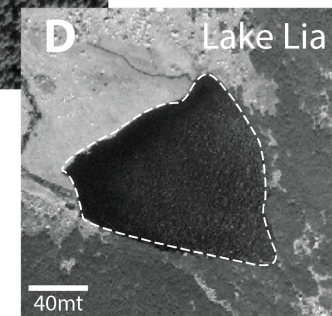
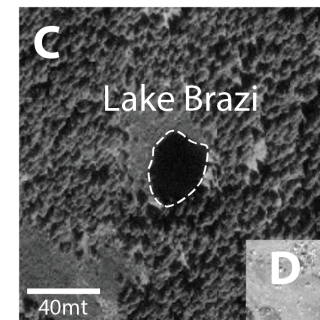
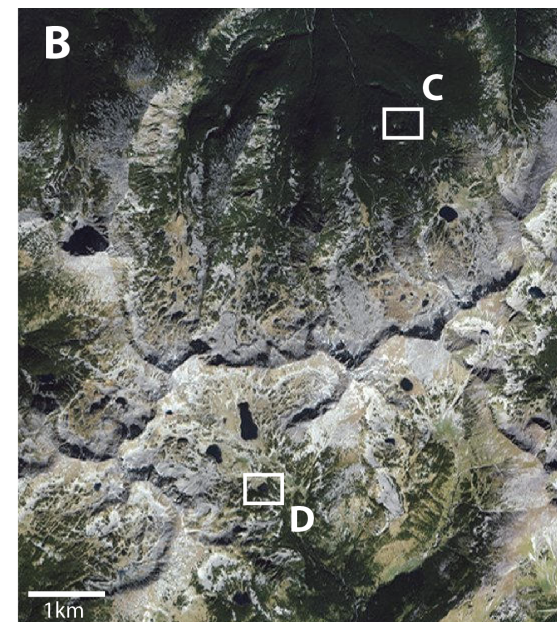
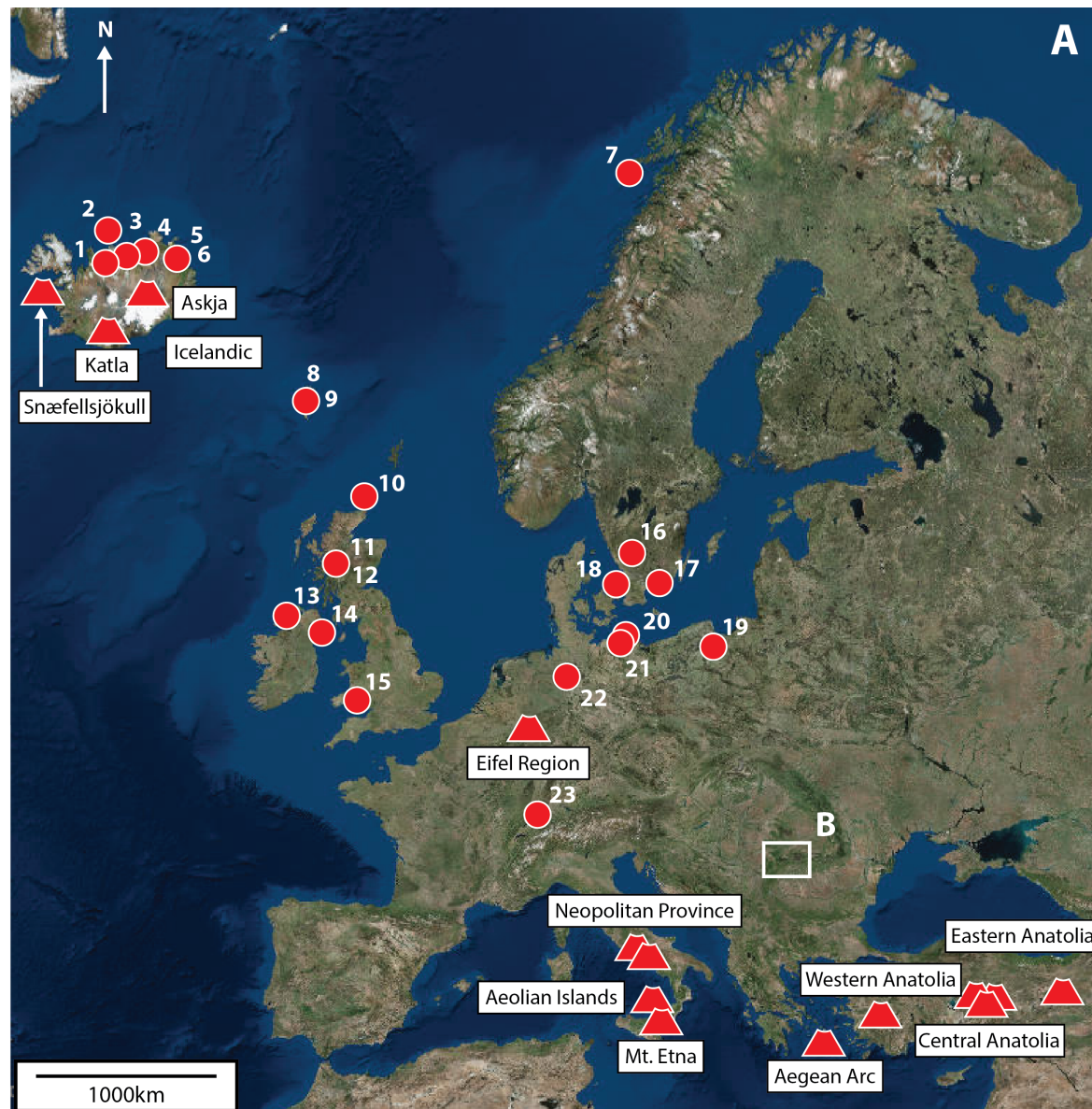
1. Introduction

The Late Glacial to Early Holocene transition (~16-8 kya) represents a period of abrupt climatic changes recorded in numerous multi-proxy palaeoenvironmental archives globally (Blockley et al., 2014; Moreno et al., 2014). These climatic changes occurred on centennial and even decadal timescales (Alley et al., 2003; Steffensen et al., 2008). Understanding the underlying driving and associated propagation mechanisms remains challenging, due to the large chronological uncertainties associated with dating methods, preventing robust inter-site comparisons of abrupt climatic transitions (Brauer et al., 2014; Bronk Ramsey et al., 2014).

The identification of widely dispersed volcanic ash (tephra) horizons can help to address these limitations (Lowe, 2011). During explosive volcanic eruptions, the fine ash component of tephra can be widely dispersed and preserved, providing time synchronous marker layers in a range of palaeoclimate records. These tephrostratigraphic markers facilitate the precise temporal comparison of disparate palaeoclimate archives (e.g. Lane et al., 2011a; Blockley et al., 2012). The identification of cryptotephra (non-visible) horizons beyond the extent of visible tephra fall layers, has enabled the application of tephrochronology over much greater areas (e.g. Jensen et al., 2014; Albert et al., 2015; van der Bilt et al., 2017). Because of this, cryptotephra horizons are becoming a powerful tool for integrating geographically disparate records, facilitating better understanding of the dynamics of abrupt climate change (e.g. Lane et al., 2013). Over the last decade, numerous European records have been subjected to detailed cryptotephra investigations, providing insights into past regional abrupt climate change, especially in northern and western Europe (e.g. Macleod et al., 2014; Lowe et al., 2015). Yet regions such as Central Eastern Europe

have been largely overlooked for cryptotephra application despite the demonstrated importance of visible distal and local tephra in providing marker horizons (Veres et al., 2013; Karátson et al., 2016). However, it is expected that the region holds significant potential for successful cryptotephra investigations due to its proximity to multiple volcanic fields, which have been active during the Late Quaternary, as well as its location at the convergence of several major air circulation patterns (Fig.1A; Haliuc et al., 2017; Longman et al., 2017a, b; Obreht et al., 2017).

Figure 1. (A) Landsat image (EU-DEM, 2016) of Europe showing the proximity of known active volcanic centres during the Late Glacial period and sites where the Askja-S tephra has been reported: 1) Skagafjörður (Sigvaldason, 2002); 2) MD99-2271 (Gudmundsdóttir et al., 2011); 3) Laufas (Sigvaldason, 2002); 4) Gjastykki (Sæmundsson, 1991); 5) Bakkaflói (Norrdahl and Hjort 1993); 6) Vopnafjörður (Sigvaldson, 2002); 7) Borge Bog (Pilcher et al., 2005); 8) Høvdarhagi Bog (Lind and Wastegård., 2011); 9) Havnardalmyren (Kylander et al., 2012); 10) Quoyloo Meadow (Timms et al., 2016); 11) Inverlair (Kelly et al., 2016); 12) Turret Bank (Lowe et al., 2017); 13) Lough Nadourcan (Turney et al., 2006); 14) Long Lough (Turney et al., 2006); 15) Pant-y-Llyn (Jones et al., 2017a); 16) Mulakullegöl (Lilija et al., 2013); 17) Hässedala port (Davies et al., 2003, Wohlfarth et al., 2006); 18) Tøvelde (Larsen, 2013); 19) Lake Czechowskie (Wulf et al., 2016b); 20) Endinger Bruch (Lane et al., 2012a); 21) Lake Tiefer See (Wulf et al., 2016b); 22) Lake Hämelsee (Jones et al., 2017b); 23) Soppensee (Lane et al., 2011b). **(B)** Landsat image of the Retezat Mountains showing Lake Brazi **(C)** and Lake Lia **(D)**.



Here, we present the important discovery of an Icelandic-derived cryptotephra, the Askja-S, within two lacustrine palaeoenvironmental records from the Southern Carpathian Mountains. This provides, for the first time, a direct tephra linkage between multi-proxy palaeoclimatic archives in south-eastern Europe with those in north-western Europe.

2. Background

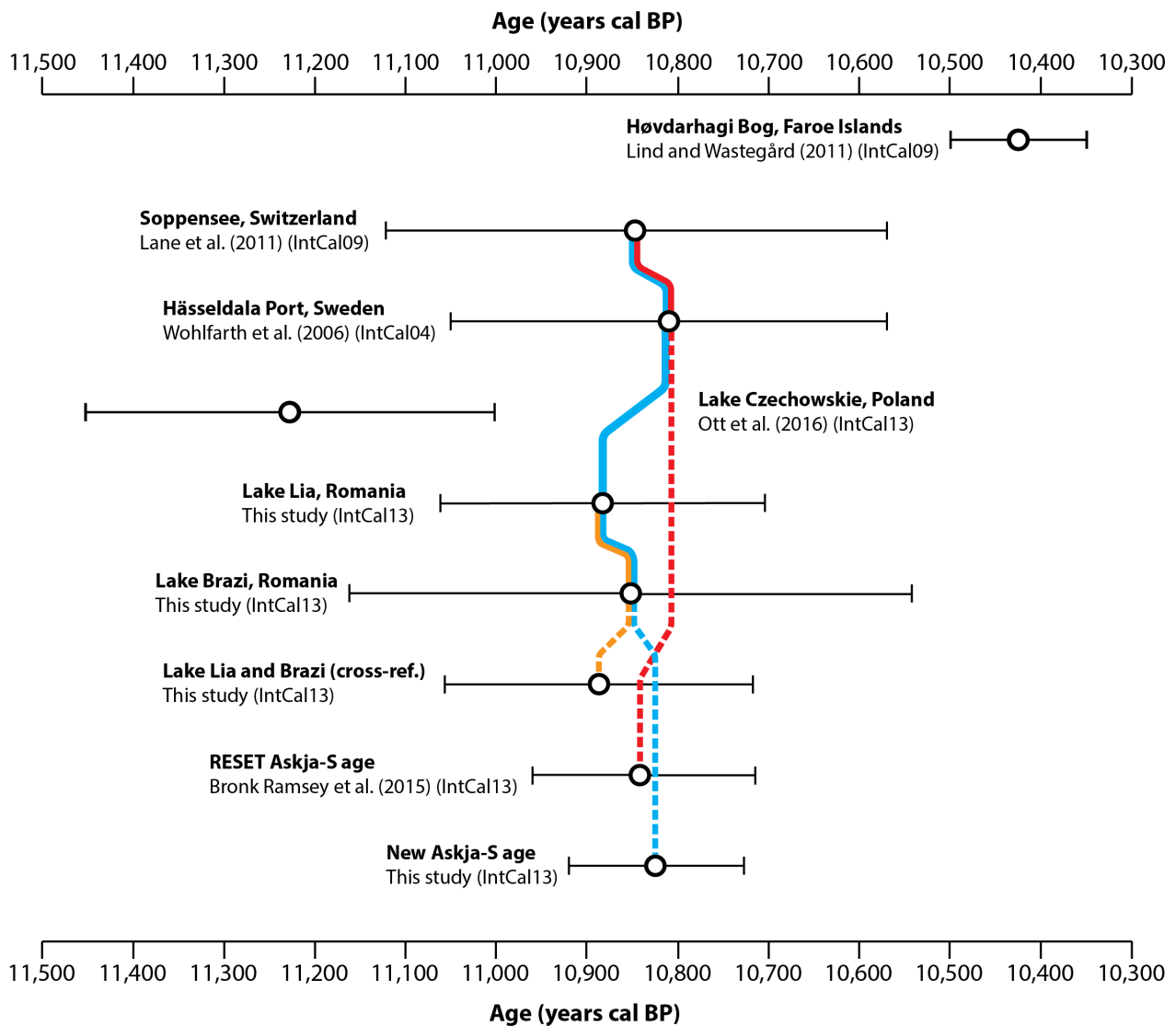
2.1. *Askja-S tephra*

The Askja-S tephra is the product of a Plinian eruption that formed the Askja caldera at the Dyngjuföll volcanic centre, Iceland (Sigvaldson, 2002). The estimated volume of this rhyolitic eruption is $1.5 \pm 0.5 \text{ km}^3$ dense-rock equivalent (DRE), relative to a Volcanic Explosivity Index (VEI) of 5 (Newhall and Self, 1982; Sigvaldson, 2002). The eruption coincided with glacial retreat in Iceland after Greenland Stadial (GS)-1. Proximal Askja-S Plinian fall deposits are distributed along the north-eastern coast of Iceland (Fig.1A, Sæmundson, 1991; Norddahl and Hjort, 1994; Sigvaldson, 2002; Gudmundsdóttir et al., 2011), confirming a dominant NNE plume dispersal off Iceland.

The Askja-S was first reported distally by Davies et al. (2003) as a cryptotephra horizon in a sediment core from Hässeldala Port, Sweden. Askja-S cryptotephra has since been observed as far north as Borge, Norway (Pilcher et al., 2005), as far east as Lake Czechowskie, Poland (Wulf et al., 2016b) and as far south as Soppensee, Switzerland (Lane et al., 2011b), limiting the Askja-S dispersal to mainly north-western European sites (Fig. 1A). Most recently, the tephra has been discovered in Pant-y-Llyn, South Wales (Jones et al., 2017a).

Several ages have been suggested for the eruption of the Askja-S (Fig. 2). At Hässeldala Port, an age of $10,810 \pm 240$ cal yrs BP was reported by Wohlfarth et al. (2006) which has since been supported by an age of $10,846 \pm 276$ cal yrs BP at Soppensee (Lane et al., 2011c, Fig.2; all dates reported in this paper are at 95.4% probability). A younger age of $10,425 \pm 75$ cal yrs BP has been suggested by Lind and Wastegård, (2011) from Høvdarhagi Bog, Faroe Islands, whilst a significantly older age of $11,228 \pm 226$ cal yrs BP has been provided by Ott et al. (2016) based on a floating varve chronology from Lake Czechowskie. Arguably, the most robust age estimate for the Askja-S tephra has been produced by Bronk Ramsey et al. (2015), through integrating radiocarbon age models from multiple palaeoenvironmental records from across Europe using the RESET (RESponse of humans to abrupt Environmental Transitions) tephra lattice, producing a refined modelled age of $10,841 \pm 115$ cal yrs BP.

Figure 2. *Schematic representation of age estimates for the Askja-S tephra from published records, and newly remodelled data from this study. The red line indicates the sites cross-referenced for the Bayesian chronological modelling of Bronk Ramsey et al. (2015) to produce a refined the Askja-S age estimate as part of the RESET tephra lattice; the orange line shows the age estimate from modelling performed in the present study, cross-referencing of Lakes Brazi and Lia only; and the blue line indicates the records that were cross-referenced to produce our preferred the new Askja-S age building upon the RESET model by Bronk Ramsey et al. (2015) with the incorporation of the data from Lakes Brazi and Lia (this study)*



141

142 2.2. Study Sites

143 The Retezat Mountains form the western massif of the Southern Carpathian Mountains.

144 This area was previously glaciated during the Last Glacial Maximum, with around 58

145 permanent glacial lakes still preserved (Magyari et al., 2009). Of these, two lakes, Brazi and

146 Lia (Fig. 1B) were selected for cryptotephra investigation due to the extensive

147 palaeoenvironmental investigations previously undertaken at both sites for the Late Glacial

148 and Early Holocene periods (e.g. Magyari et al., 2012; Tóth et al., 2015; Buczkó et al., 2013;

Orbán et al., 2017; Vincze et al., 2017). The chronologies of both sites are based upon radiocarbon (^{14}C) dating (Magyari et al., 2009, 2012; Hubay et al., 2016; Pál et al., 2016).

Lake Brazi (45°23'47" N, 22°54'06" E, 1740m a.s.l., Fig. 1C) is located on the northern slope of the Retezat Mountains in a former kettle-hole setting (Magyari et al., 2009). Lake Lia (45°21'7.3" N, 22°52'27.0" E, 1910m a.s.l., Fig. 1D) is a small, shallow lake located 5km from Lake Brazi on the south facing slopes of the Retezat Mountains (Orbán et al., 2017; Vincze et al., 2017).

3. Methods

3.1. *Tephra sample preparation*

Contiguous 5cm resolution samples were taken across the sedimentologically identified Late Glacial to Early Holocene sequence of both Lake Brazi (TDB) and Lia (LIA) sediment cores (Magyari et al., 2009; Vincze et al., 2017). The glass shards were extracted following the density separation procedures described by Turney (1998) and Blockley et al. (2005) with a single modification where samples were sieved at 80 μm and 15 μm , rather than 80 μm and 25 μm . The tephra extraction residue (2.55g cm $^{-3}$) of each sample was mounted on to microscope slides in Canada Balsam. Volcanic glass shards were identified and counted under a high-powered, polarizing optical microscope. Where peaks in glass shard concentration were identified at 5cm resolution, these depths were re-sampled at a higher resolution (1cm) and prepared as above.

Individual glass shards from identified peaks were concentrated and mounted on to epoxy resin stubs with the use of a micromanipulator (see Lane et al., 2014). Finally, the shards were sealed in resin, sectioned and polished for geochemical analyses.

3.2. Geochemical analysis

Major and minor element compositions of individual glass shards were measured using a JEOL-8600 wavelength-dispersive electron microprobe (WDS-EPMA) at the Research Laboratory for Archaeology and History of Art, University of Oxford. All analyses used an accelerating voltage of 15 kV, beam current of 6 nA and 10 μm -diameter beam. Peak counting times were 30 seconds for all elements apart from Na (12s), Mn (40s), Cl (50s) and P (60s). The electron microprobe was calibrated using a suite of mineral standards, and the PAP absorption correction method was used for quantification. The accuracy and precision of our analyses were assessed using analyses of the MPI-DING reference glasses (Jochum et al., 2006), which were run alongside the unknown tephra samples. Data were filtered to remove accidental analyses of minerals and biogenic silica. Volcanic glass with analytical totals <95% were also removed.

3.3. Age-depth modelling

The original radiocarbon dates from both Lake Brazi and Lake Lia (Magyari et al., 2009, 2012; Hubay et al., 2016; Pál et al., 2016) have been re-modelled using the Bayesian statistical program OxCal (version 4.3, Bronk Ramsey, 2017) applying the IntCal13 calibration curve (Reimer et al., 2013). A 'P_Sequence' deposition model (Bronk Ramey,

2009a) was applied for both sites utilising a variable k parameter to allow OxCal to independently determine the optimal variability in sedimentation rate (Bronk Ramsey and Lee, 2013). A 'general' *Outlier_Model* was applied with a 5% prior probability of any individual date being a statistical outlier (Bronk Ramsey, 2009b).

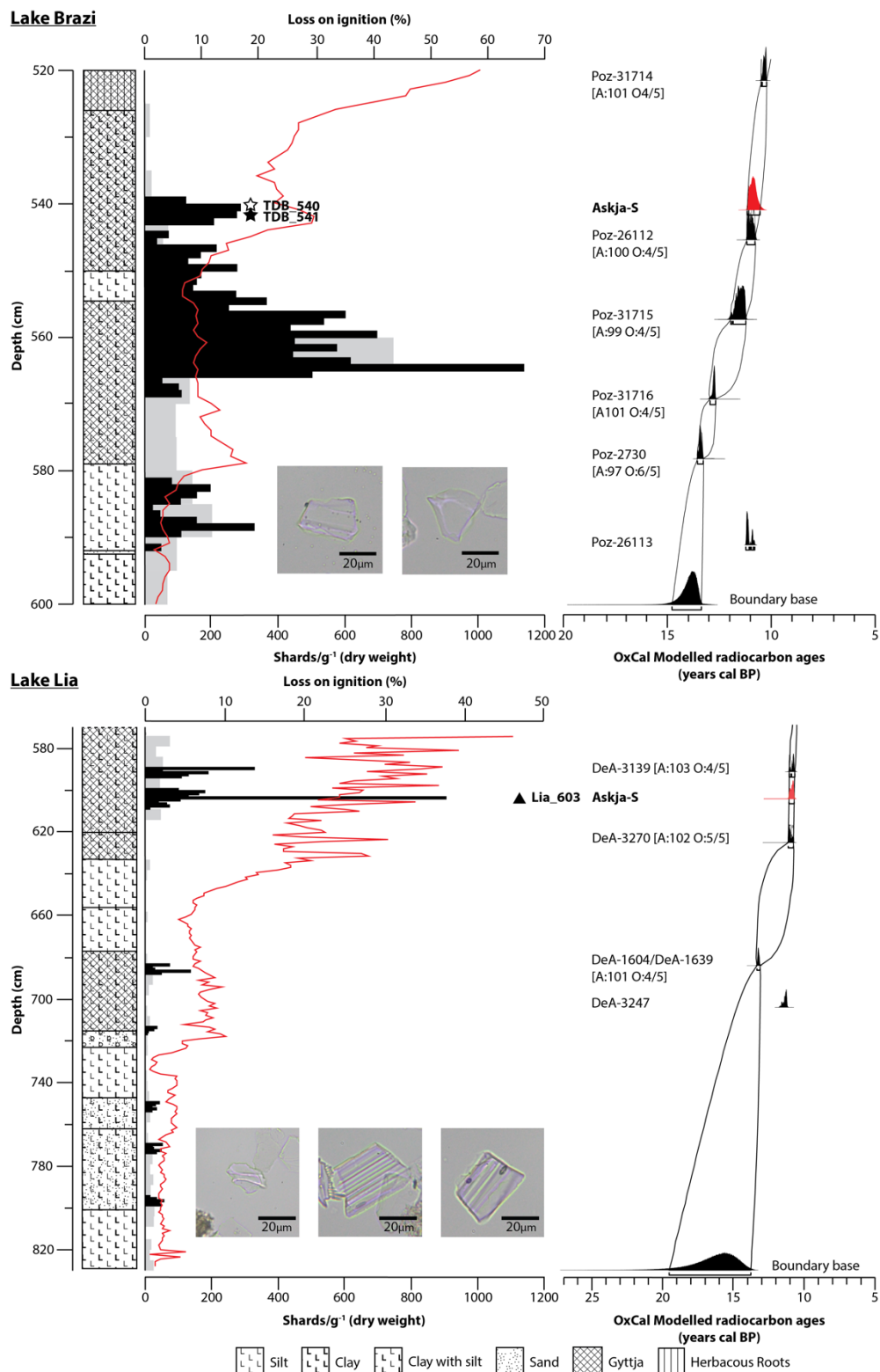
4. Results and discussion

4.1. *Position and identification of cryptotephra layers*

Distinct peaks in tephra shard concentration were identified in both the Lake Brazi and Lia sediment cores (Fig. 3). Robust geochemical analysis identified separate eruptions by minor and major element comparisons. For the purposes of this contribution we only present grain-specific glass geochemistry from selected peaks in glass shard concentrations in the Late glacial – early Holocene sequences of the two lakes, at 540/541 cm from the Lake Brazi sedimentary sequence (TDB_540, 288 shards g^{-1} ; and TDB_541, 275 shards g^{-1}) and 603 cm in the Lake Lia record (LIA_603, 908 shards g^{-1}) (Fig. 3). Due to the nearly identical shard concentrations across TDB_540 and TDB_541, the positioning of the peak or isochron is taken as the mid-point of these depths (540.5cm). Other peaks in tephra shard concentrations, with different geochemical characteristics from the distinctive Askja-S, will be discussed in future publications.

Figure 3. *Lithostratigraphy, loss-on-ignition, total shard concentration (from low-resolution, 5cm contiguous scans, light grey; and from higher, 1cm resolution scans, black) and re-modelled age-depth models for both Lake Brazi and Lake Lia focusing on the Late Glacial and*

213 Early Holocene core sections. The peaks containing the Askja-S tephra that are only
 214 discussed in this paper are highlighted. Other tephra concentration peaks will be the subject
 215 of future publications. Images of individual tephra shards from these Askja-S peaks are
 216 shown.



TDB_540/541 and LIA_603 are positioned within the locally described pollen zones associated with the transition from the Younger Dryas to Early Holocene (Magyari et al., 2009, 2012; Vincze et al., 2017). The modelled age of Askja-S from Lake Brazi is $10,852 \pm 309$ cal yrs BP and Lake Lia $10,885 \pm 183$ cal yrs BP (Fig.3), within good statistical agreement of each other.

The shard morphologies of both layers exhibit a similar fluted appearance, the shards are colourless, with a maximum shard size of 20-25 μ m (Fig.3). The individual geochemical analyses of the glass shards in TDB_540/541 and LIA_603 are presented in Table 1, with selected major and minor element bi-plots shown in Figure 4. TDB_540/541 and LIA_603 demonstrate a homogenous, rhyolitic glass composition characterised by low K₂O (TDB_540/541: 2.60 ± 0.05 wt. %, LIA_603: 2.60 ± 0.06 wt. %; 1 s.d.) and high CaO (TDB_540/541: 1.65 ± 0.11 wt. %; LIA_603: 1.61 ± 0.06 wt %; 1 s.d.). Due to this distinctive glass chemistry and the chronostratigraphic position of the TDB_540/541 and LIA_603 samples, we can confidently correlate them to the Askja-S erupted from the Dyngjuföll volcanic centre, Iceland (Sigvaldson, 2002) as well as to identified distal occurrences of ash from this eruption at multiple sites across north–western Europe (Davies et al., 2003; Pilcher et al., 2005; Lane et al., 2011b; Wulf et al., 2016b; Jones et al., 2017b) (Fig 1A, Fig 4). The ultra-distal discovery of the Askja-S tephra, over 3000 km from volcanic source in the Southern Carpathian Mountains dramatically extends the known dispersal of fine ash (typically < 25 μ m glass shards) from this Plinian eruption and, furthermore, represents the first identification of an Icelandic tephra in south-eastern Europe.

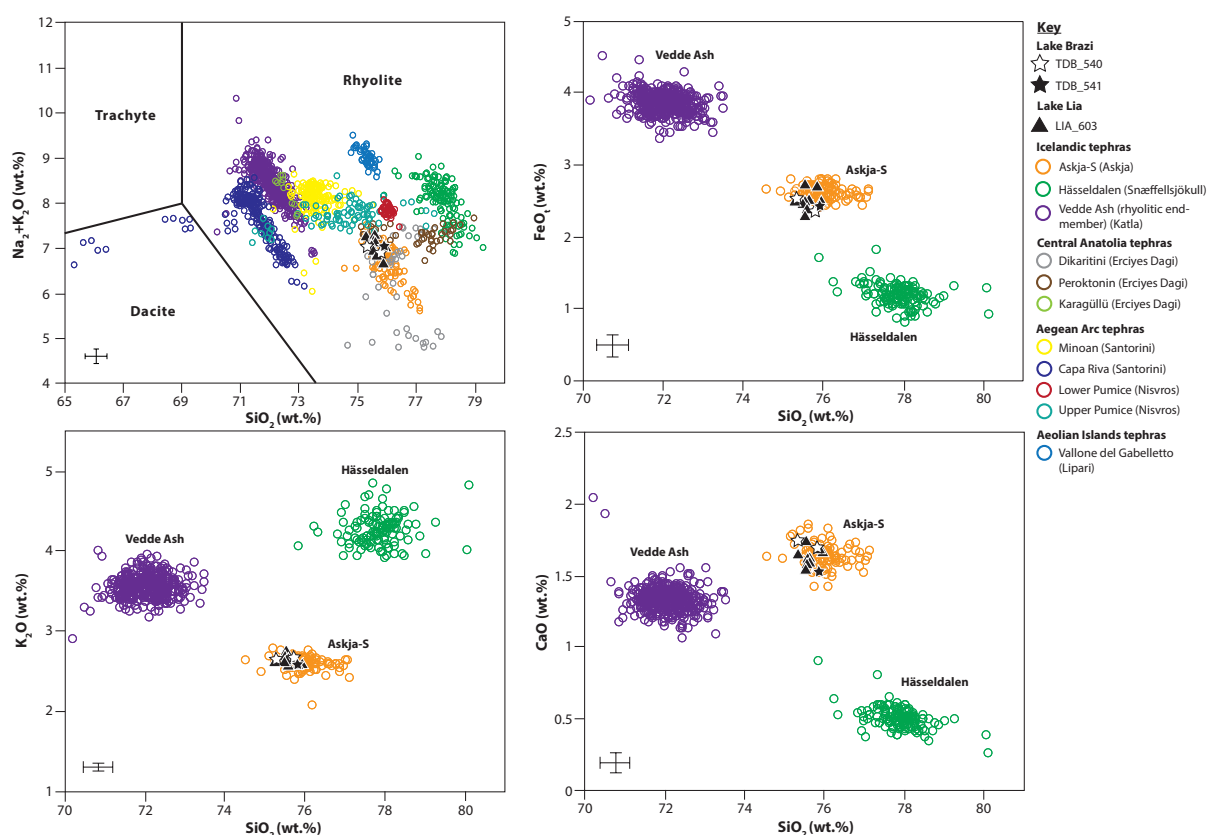
240 **Table 1.** Major element glass compositions (normalised to 100%), along with raw (non-
241 normalised) analytical totals of individual tephra shards from Lake Brazi (TDB_540,
242 TDB_541) and Lake Lia (LIA_603). Unnormalised data can be seen in Supplementary
243 Material A.

	Sample	SiO ₂	TiO ₂	Al ₂ O ₃	FeO _t	MnO	MgO	CaO	Na ₂ O	K ₂ O	P ₂ O ₅	Cl	Analytical Total
	TDB_540	75.35	0.34	12.37	2.63	0.16	0.26	1.73	4.42	2.61	0.05	0.08	95.89
		75.82	0.3	12.54	2.47	0.06	0.24	1.68	4.17	2.64	0.03	0.05	98.08
	TDB_541	75.93	0.34	12.23	2.52	0.12	0.23	1.53	4.48	2.54	0.01	0.07	97.04
	Mean	75.7	0.33	12.38	2.54	0.11	0.24	1.65	4.36	2.6	0.03	0.07	97
	SD (1σ)	0.31	0.02	0.15	0.08	0.05	0.02	0.11	0.16	0.05	0.02	0.01	1.09
	LIA_603	75.56	0.34	12.49	2.6	0.16	0.25	1.52	4.26	2.63	0.07	0.11	98.58
		75.32	0.29	12.42	2.61	0.14	0.27	1.63	4.63	2.59	0.04	0.08	98.48
244		75.66	0.28	12.56	2.62	0.09	0.25	1.61	4.26	2.54	0.05	0.08	97.27
		75.53	0.27	12.41	2.58	0.05	0.29	1.72	4.4	2.59	0.07	0.09	99.3
		75.59	0.26	12.48	2.41	0.1	0.26	1.57	4.5	2.74	0.02	0.06	98.3
245		75.9	0.29	12.28	2.79	0.13	0.24	1.66	4.09	2.53	0.01	0.08	99.94
		75.6	0.3	12.21	2.82	0.06	0.21	1.6	4.49	2.62	0.02	0.08	98.73
		75.63	0.33	12.36	2.49	0.16	0.24	1.58	4.47	2.61	0.06	0.07	99.87
		75.98	0.27	12.01	2.62	0.07	0.27	1.65	4.41	2.55	0.08	0.1	98.74
	Mean	75.64	0.29	12.36	2.62	0.11	0.25	1.61	4.39	2.6	0.05	0.08	98.8
	SD (1σ)	0.2	0.03	0.17	0.13	0.04	0.02	0.06	0.16	0.06	0.03	0.02	0.82

246

247 **Figure 4.** Geochemical bi-plots of the major elemental data from Lake Brazi and Lake Lia
248 with known rhyolitic eruptions during the Late Glacial to Early Holocene from volcanic
249 sources close to the sites. Reference data for tephras are from Central Anatolia (Hamann et
250 al., 2010, Cullen et al., 2014, Tomlinson et al., 2015), Aegean Arc (Eastwood et al., 1999,
251 Kwiecien et al., 2008, Tomlinson et al., 2012, 2015, Cullen et al., 2014), Aeolian Islands
252 (Albert et al., 2017) and Icelandic tephra (Vedde Ash: Birks et al., 1996, Wastegård et al.,
253 1998, 2000, Turney et al., 1997, 2006, Raner et al., 2005, Pilcher et al., 2005, Davies et al.,
254 2005, Blockley et al., 2007, Lane et al., 2011b, c, d, 2012a, b; Hässeldalen: Lane et al.,
255 2012b, Housley et al., 2013, Davies et al., 2003, Lind and Wastegård, 2011, Liljn et al., 2013,
256 Larsen and Noe-Nygaard., 2014, Wulf et al., 2016b; and Askja-S: Sigvaldason 2002, Davies et
257 al., 2003, Turney et al., 2006, Lane et al., 2011b, Lind and Wastegard, 2011, Wulf et al.,

2016, Kelly et al., 2016, Jones et al., 2017b, Lowe et al., 2017). Error bars presented are 2
 standard deviations of repeat analysis of the StHs6/80-G MPI-DING standard glass.



260

261 4.2. Chronological modelling

262 Owing to the occurrence of the Askja-S in both lake records, its eruption age can be
 263 subsequently refined using cross-referencing in OxCal (Bronk Ramsey, 2009a), producing an
 264 updated age of $10,889 \pm 174$ cal yrs BP for the deposition of this tephra within both lake
 265 records. This is within statistical agreement with the Askja-S age proposed by Bronk Ramsey
 266 et al. (2015), but contradicts the older and younger ages reported by Ott et al. (2016) and
 267 Lind and Wastegård (2011), respectively. Whilst other, younger tephra from Askja volcano
 268 have been reported (e.g. the Askja-L and Askja-H; Jóhannsdóttir, 2007, Striberger et al.,
 269 2012, Gudmundsdóttir et al., 2016), there is no evidence to date of these tephra having

been identified beyond Iceland. Therefore, we presume that the divergent ages presented by Ott et al. (2016) and Lind and Wastegård (2011) are the result of problematic site chronologies, rather than the misattribution of these tephra layers.

Combining the chronological modelling of the Askja-S tephra in Lakes Brazi and Lia with the data from the other two sites, Soppensee and Hässeldala Port whose ages for the tephra are within statistical agreement with our own, improves upon the age estimate of the RESET tephra lattice by Bronk Ramsey et al. (2015, Fig.2). The new results from the model provide a refined age of $10,824 \pm 97$ cal yrs BP (Fig.2).

~~5. Implications~~ 5. Future research

5.1. *Palaeoenvironments interpretation*

The discovery of an Icelandic tephra layer in two palaeoenvironmental records from the Southern Carpathians provides a key tephrostratigraphic linkage between western and northern Europe with south-eastern Europe (Fig. 1). Here it is particularly important as the Askja-S tephra is chrono-stratigraphically positioned in the Early Holocene close to where several abrupt climatic transitions have been reported, for instance the Preboreal Oscillation (PBO, 11.5-11.4 b2k,) and the '10.7 kya event' which are identified in numerous European palaeoclimate records (Björck et al., 1997; Wohlfarth et al., 2006; Lowe et al., 2015; Ott et al., 2016). However, these events remain somewhat poorly understood in terms of their environmental impacts and geographical expression (e.g. Björck et al., 1996, 1997; Wohlfarth et al., 2006). Both lakes, have undergone high-resolution, multi-proxy

palaeoenvironmental investigations across this time period (e.g. Magyar et al., 2012; Buczkó et al., 2013; Tóth et al., 2015, in press; Pál et al., 2016, in press, Finsinger et al., 2014, in press; Vincze et al., 2017). The additional identification of the Askja-S within both records, provides an ideal opportunity to investigate comparative environmental dynamics and duration of the PBO through improving chronological modelling from north-western Europe to the Southern Carpathians.

5.2. ~~Potential for~~ Expansion of tephrostratigraphic frameworks

This finding demonstrates that the Askja-S tephra provides a powerful tephrostratigraphic marker extending from north-west Europe to south-eastern Europe. The identification of this cryptotephra horizon is not uniform across north-west European sites that have undergone detailed cryptotephra investigations, revealing a patchy distribution of this ash fall event (Jones et al., 2017a).

A number of factors could be responsible for the distal occurrences of this widespread ash dispersal from Iceland. Following an initial NNE plume dispersal off Iceland, evident in proximal deposits (Sæmundsson, 1991; Norddahl and Hjort 1993; Sigvaldason, 2002), the resulting complex distribution of ash fall evidenced across Europe may have been governed by the variable/evolving concomitant weather patterns, or different atmospheric circulation at changing heights in the plume. Modern Icelandic eruptions have exhibited complicated dispersals following their initial dispersals away from Iceland, seemingly affected by these factors (e.g. Davies et al., 2010; Gudmundsson et al., 2012).

The 15 μm sieve mesh size used here was crucial to the retention and identification of the finest grain ash particles produced during this eruption ($<25\ \mu\text{m}$). Typically in previous studies a 25 μm mesh was employed and may be responsible for the Askja-S fine-grain material not being recovered by the cryptotephra procedures employed. Therefore, our findings provide encouragement for re-investigations of the temporally relevant sediments at these sites. Speculatively, the concentration of Askja-S tephra in the Lake Brazi and Lia records could have been influenced by orographic precipitation induced by the Carpathian mountain range. Additional factors such as regional bias of cryptotephra investigations (Watson et al., 2017), site-specific sedimentary taphonomic processes (Pyne-O'Donnell, 2011) and lack of continuous high-resolution cryptotephra searches (Timms et al., 2016) may all have acted to limit the currently known spatial distribution of this tephrostratigraphic marker in Europe.

Crucially, the identification of Icelandic tephra in Lake Brazi and Lake Lia, which are geographically closer to other productive volcanic regions (e.g. Italian, Aegean and Anatolian volcanoes), highlights the enormous potential of these sites for the future integration of regional tephrostratigraphic frameworks from multiple volcanic sources.

Acknowledgements

RK is funded by the UK National Environmental Research Council (NERC; grants: NE/L002612/1) as part of the Environmental Research Doctoral Training Program at the University of Oxford. PGA and RAS are supported by Early Career Fellowships from the Leverhulme Trust (grants: ECF-2014-438 and ECF-2015-396). Drilling and palaeoenvironmental study of Lake Brazi and Lake Lia was supported by the Hungarian OTKA grant NF 101362 and GINOP-2.3.2-15-2016-00009. EU-DEM map produced using

336 Copernicus data and information funded by the European Union – EU-DEM layers. The
337 authors would like to thank Simon Blockley and an anonymous reviewers for their
338 comments and feedback.

339

340 **Supplementary material A: Raw geochemical data**

341 **Supplementary material B: OxCal coding**

342

343 **References**

344 Albert, P.G., Hardiman, M., Keller, J., Tomlinson, E.L., Smith, V.C., Bourne, A.J., Wulf, S.,
345 Zanchetta, G., Sulpizio, R., Müller, U.C., Pross, J., Ottolini, L., Matthews, I.P., Blockley, S.P.E.,
346 Menzies, M.A., 2015. Revisiting the Y-3 tephrostratigraphic marker: a new diagnostic glass
347 geochemistry, age estimate, and details on its climatostratigraphical context. Quaternary
348 Science Reviews 118, 105-121.

349 Albert, P.G., Tomlinson, E.L., Smith, V.C., Traglia, F.D., Pistolesi, M., Morris, A., Donato, P.,
350 Rose, R.D., Sulpizio, R., Keller, J., Rosi, M., Menzies, M., 2017. Glass geochemistry of
351 piroclastic deposits from the Aeolian Islands in the last 50ka: A proximal database for
352 tephrochronology. Journal of Volcanology and Geothermal Research 33, 81-107.

353 Alley, R.B., Marotzke, J. and Nordhaus, W.D., 2003. Abrupt climate change. Science 299,
354 2005–2010.

355 Birks, H.H., Guliksen, S., Hafliðason, H., Mangerud, J., Possnert, G., 1996. New radiocarbon

356 dates for the Vedde Ash and the Saksunarvatn ash from western Norway. Quaternary
357 Research 45:2, 119-127.

358 Björck, S., Kromer, B., Johnsen, S., Bennike, O., Hammarlund, D., Lemdahl, G., Possnert, G.,
359 Rasmussen, T.L., Wohlfarth, B., Hammer, C.U., Spurk, M., 1996. Synchronized terrestrial
360 Atmospheric deglacial records around the north Atlantic. Science 274, 1155-1160.

361 Björck, S., Rundgren, M., Ingolfsson, O., Funder, S., 1997. The Preboreal oscillation around
362 the Nordic Seas: terrestrial and lacustrine responses. Journal of Quaternary Science 12, 455-
363 465.

364 Blockley, S.P.E., Donnell, S.D.F.P., Lowe, J.J., Matthews, I.P., Stone, A., Pollard, A.M., Turney,
365 C.S.M., Molyneux, E.G., 2005. A new and less destructive laboratory procedure for the
366 physical separation of distal glass tephra shards from sediments. Quaternary Science
367 Reviews 24, 1952– 1960.

368 Blockley, S.P.E., Lane, C.S., Lotter, A.F., Pollard, A.M., 2007. Evidence for the presence fo the
369 Vedde Ash in central Europe. Quaternary Science Reviews 26:25-28, 3030-3036.

370 Blockley, S.P.E., Lane, C.S., Hardiman, M., Rasumssen, S.O., Seierstad, I.K., Steffensen, J.P.,
371 Svensson, A., Lotter, A.F., Turney, C.S.M., Bronk Ramsey, C., 2012. Synchronisation of
372 palaeoenvironmental records over the last 60,000 years, and an extended INTIMATE event
373 stratigraphy to 48,000 b2k. Quaternary Science Reviews 36, 2-10.

374 Blockley, S.P.E., Bourne, A., Brauer, A., Davies, S., Hardiman, M., Harding, P., Lane, C.,
375 MacLeod, A., Matthews, I., Pyne-O'Donnell, S., Wulf, S., Zanchetta, G., 2014.

376 Tephrochronology and the extended INTIMATE (integration of ice-core, marine and

377 terrestrial records) event stratigraphy 8-128ka b2k. Quaternary Science Reviews 106, 88-
378 100.

379 van der Bilt, W.G.M., Lane, C.S., Bakke, J. 2017. Ultra-distal Kamchatkan ash on Artic
380 Svalbard: Towards hemispheric cryptotephra correlation. Quaternary Science Reviews 164,
381 230-235.

382 Brauer, A., Hajdas, I., Blockley, S.P.E., Bronk Ramsey, C., Christl, M., Ivy-Ochs, S., Moseley, G.
383 E., Nowaczyk, N.N., Rasmussen, S.O., Roberts, H.M., Spötl, C., Staff, R.A., Svensson, A., 2014.
384 The importance of independent chronology in integrating records of past climate change for
385 the 60–8 ka INTIMATE time interval. Quaternary Science Reviews 106, 47–66.

386 Bronk Ramsey, C., 2009a. Bayesian analysis of radiocarbon dates. Radiocarbon 51, 337–360.

387 Bronk Ramsey, C., 2009b. Dealing with outliers and offsets in radiocarbon dating.
388 Radiocarbon 51:3, 1023-1045.

389 Bronk Ramsey, C., 2017. OxCal Project, Version 4.3. Retrieved April 2017. [https://c14.](https://c14.arch.ox.ac.uk/oxcal/OxCal.html)
390 [arch.ox.ac.uk/oxcal/OxCal.html](https://c14.arch.ox.ac.uk/oxcal/OxCal.html).

391 Bronk Ramsey, C., Lee, S. 2013. Recent and planned developments of the program
392 OxCal. Radiocarbon 55, 3-4.

393 Bronk Ramsey, C., Albert, P., Blockley, P., Hardiman, M., Lane, C., Maclead, A., Matthews,
394 I.P., Muscheler, R., Palmer, A., Staff, R.A., 2014. Integrating timescales with time-transfer
395 functions: a practical approach for an INTIMATE database. Quaternary Science Reviews 106,
396 67-80.

397 Bronk Ramsey, C., Albert, P.G., Blockley, S.P.E., Hardiman, M., Housley, R.A., Lane, C.S., Lee,

398 S., Matthews, I.P., Smith, V.C., Lowe, J.J., 2015. Improved age estimates for key Late
 399 Quaternary European tephra horizons in the RESET lattice. *Quaternary Science Reviews* 118,
 400 18–32.

401 Buczkó, K., Magyari, E.K., Braun, M., Bálint, M., 2013. Diatom-inferred lateglacial and
 402 Holocene climatic variability in the South Carpathian Mountains (Romania). *Quaternary*
 403 *International* (Advancing Pleistocene and Holocene climate change research in the
 404 Carpathian-Balkan region) 293, 123–135.

405 Cullen, V.L., Smith, V.C., Arz, H.W. 2014. The detailed tephrostratigraphy of a core from the
 406 south-east Black Sea spanning the last ~60ka. *Journal of Quaternary Science* 29:7, 675-690.

407 Davies, S.M., Wastegård, S., Wohlfarth, B., 2003. Extending the limits of the Borrobol Tephra
 408 to Scandinavia and detection of new early Holocene tephras. *Quaternary Research* 59, 345–
 409 352.

410 Davies, S.M., Hoek, W.Z., Bohncke, S.J.P., Lowe, J.J., O'Donnell, S.P., Turney, C.S.M., 2005.
 411 Detection of Lateglacial distal tephra layers in the Netherlands. *Boreas* 34:2, 123-135.

412 Davies, S.M., Larsen, G., Wastegård, S., Turney, C.S., Hall, V.A., Coyle, L., Thordarson, T.
 413 2010. Widespread dispersal of Icelandic tephra: how does the Eyjafjöll eruption of 2010
 414 compare to past Icelandic events? *Journal of Quaternary Science* 25:5, 605-611.

415 Eastwood, W.J., Pearce, N.J.G., Westgate, J.A., Perkins, W.T., Lamb, H.F, Roberts, N., 1999.
 416 Geochemistry of Santorini tephra in lake sediments from southwest Turkey. *Global and*
 417 *Planetary Change*, 21:1-3, 17-29.

418 Finsinger, W., Kelly, R., Fevre, J., Magyari, E.K. 2014. A guide to screening charcoal peaks in
419 macrocharcoal-area records for fire-episode reconstructions. *Holocene* 24: 1002-1008.

420 Finsinger, W., Fevre, J., Orbán, I., Pál, I., Vincze, I., Hubay, K., Birks, H.H., Braun, M., Tóth, M.,
421 Magyari, E.K., In press. Holocene fire-regime changes near the treeline in the Retezat Mts.
422 (Southern Carpathians, Romania). *Quaternary International* doi: 10.1016/j.quaint.
423 2016.04.029.

424 Gudmundsdóttir, E.R., Eiríksson, J., Larsen, G., 2011. Identification and definition of primary
425 and reworked tephra in Late Glacial and Holocene marine shelf sediments off North Iceland.
426 *Journal of Quaternary Science* 26:6, 589-602.

427 Gudmundsdóttir, E.R., Larsen, G., Björck, S., Ingólfsson, Ó., Striberger, J., 2016. A new high-
428 resolution Holocene tephra stratigraphy in eastern Iceland: improving the Icelandic and
429 North Atlantic tephrochronology. *Quaternary Science Reviews* 150, 234–249.

430 Gudmundsson, M.T., Thordarson, T., Höskuldsson, Larsen, G., Björnsson, H., Prata, F.J.,
431 Oddsson, B., Magnússon, E., Högnadóttir, Petersen, G.N., Hayward,, C.L., Stevenson, J.A.,
432 Jónsdóttir, I. 2012. Ash generation and distribution from the April-May 2010 eruption of
433 Eyjafjallajökull, Iceland. *Scientific Reports* 2:572, 1-12.

434 Hamann, Y., Wulf, S., Ersoy, O., Ehrmann, W., Aydar, E., Schmiedl, G. 2010. First evidence of
435 a distal Early Holocene ash layer in eastern Mediterranean deep-sea sediments derived from
436 the Anatolian volcanic province. *Quaternary Research* 73, 497–506.

437 Haliuc, A., Veres, D., Brauer, A., Hubay, K., Hutchinson, S.M., Begy, R., Braun, M., 2017.
438 Palaeohydrological changes during the mid and late Holocene in the Carpathian area,
439 central-eastern Europe. *Global and Planetary Change* 152, 99-114.

440 Housley, R., MacLeod, A., Nalepka, D., Jurochnik, A., Masojc, M., Davies, L., Lincoln, P., Bronk
441 Ramsey, C., Gamble, C.S., Lowe, J.J., 2013. Teprostratigraphy of a Lateglacial lake sediment
442 sequence at Węgliny, southwest Poland. *Quaternary Science Reviews* 77, 4-18.

443 Hubay, K., Molnár, M., Orbán, I., Braun, M., Biro, T. and Magyari, E. 2016. Age-depth
444 relationship and accumulation rates in four sediment sequences from the Retezat Mts,
445 South Carpathians (Romania). *Quaternary International*, in press, 1–12.
446 <https://doi.org/10.1016/j.quaint.2016.09.019>

447 Jensen, B.J.L., Pyne-O'Donnell, S., Plunkett, G., Froese, D.G., Hughes, P.D.M., Sigi, M.,
448 McConnell, J.R., Amesbury, M.J., Blackwell, P.G., van den Bogaard, C., Buck, C.E., Charman,
449 D.J., Clague, J.J., Hall, V.A., Koch, J., Mackay, H., Mallon, G., McColl, L., Pilcher, J.R., 2014.
450 Transatlantic distribution of the Alaskan White River Ash. *Geology* 42:10, 875-878.

451 Jochum, K.P., Stoll, B., Herwig, K., Willbold, M., Hofmann, A.W., Amini, M., et al., 2006. MPI-
452 DING reference glasses for in situ microanalysis: new reference values for element
453 concentrations and isotope ratios. *Geochemistry, Geophysics, Geosystems* 7, 2.

454 Jóhannsdóttir, G., 2007. Mid Holocene to Late Glacial Tephrochronology in West Iceland as
455 Revealed in Three Lacustrine Environments, MS Thesis in Geology. University of Iceland.

456 Jones, G., Davies, S.M., Farr, G., Bevan, J., 2017a. Identification of the Askja-S Tephra in a
457 rare turlough record from Pant-y-Llyn, south Wales. *Proceedings of the Geologists'*
458 *Association*, 605, 1-9.

459 Jones, G., Lane, C.S., Brauer, A., Davies, S.M., de Bruijn, R., Engels, S., Haliuc, A., Hoek, W.Z.,
460 Merkt, J., Sachse, D., Turner, F., Wagner-Cremer, F., 2017b. The Lateglacial to early

461 Holocene tephrochronological record from Lake Hämerlsee, Germany: a key site within the
462 European tephra framework. *Boreas*, in press, DOI: 10.1111/bor.12250.

463 Karátson, D., Wulf, S., Veres, D., Magyari, E.K., Gertisser, R., Timar-Gabor, A., Novothny, A.,
464 Telbisz, T., Szalai, Z., Anechitei-Deacu, V., Appelt, O., Bormann, M., Janosi, C., Hubay, K.,
465 Schaebitz, F., 2016. The latest explosive eruptions of Ciomadul (Csomad) volcano, East
466 Carpathians - A tephrostratigraphic approach for the 51-29 ka BP time interval. *Journal of*
467 *Volcanology and Geothermal Research* 319, 29–51.

468 Kelly, T.J., Hardiman, M., Lovelady, M., Lowe, J.J., Matthews, I.P., Blockley, S.P.E., 2016.
469 Scottish early Holocene vegetation dynamics based on pollen and tephra records from
470 Inverlair and Loch Etteridge, Inverness-shire. *Proceedings of the Geologists' Association* 128,
471 125–135.

472 Kwiecien, O., Arz, H.W., Lamy, F., Wulf, S., Bahr, A., Rohl, U., Haug, G.H., 2008, Estimated
473 reservoir age of the Black Sea since the Last Glacial. *Radiocarbon* 50, 99-118.

474 Kylander, M.E., Lind, E.M., Wastegård, S., Löwemark, L., 2012. Recommendations for using
475 XRF core scanning as a tool in tephrochronology. *Holocene* 22, 371–375.

476 Lane, C.S., Andrič, M., Cullen, V.L., Blockley, S.P.E., 2011a. The occurrence of distal Icelandic
477 and Italian tephra in the Lateglacial of Lake Bled, Slovenia. *Quaternary Science Reviews* 30,
478 1013-1018.

479 Lane, C.S., Blockley, S.P.E., Bronk Ramsey, C., Lotter, A.F., 2011b. Tephrochronology and
480 absolute centennial scale synchronisation of European and Greenland records for the last
481 glacial to interglacial transition: a case study of Soppensee and NGRIP. *Quaternary*
482 *International* 246, 145–156.

483 Lane, C.S., Blockley, S.P.E., Lotter, A.F., Finsinger, W., Filippi, M.L., Matthews, I.P., 2011c. A
484 regional tephrostratigraphic framework for central and southern European climate archives
485 during the Last Glacial to Interglacial transition: comparisons north and south of the Alps.
486 Quaternary Science Reviews 36, 50-58.

487 Lane, C.S., De Klerk, P., Cullen, V.L., 2012a. A tephrochronology for the Lateglacial
488 palynological record of the Endinger Bruch (Vorpommern, north-east Germany). Journal of
489 Quaternary Science 27, 141–149.

490 Lane, C.S., Blockley, S.P.E., Mangerud, J., Smith, V.C., Lohne, Ø. S., Tomlindon, E. L.,
491 Matthews, I.P. Lotter, A.F. 2012b. Was the 12.1ka Iceland Vedde Ash one of a kind?
492 Quaternary Science Reviews 33, 87-99.

493 Lane, C.S., Brauer, A., Blockley, S.P.E. and Dulski, P., 2013b. Volcanic ash reveals time-
494 transgressive abrupt climate change during the Younger Dryas. Geology 41:12, 1251–1254.

495 Lane, C.S., Cullen, V.L., White, D., Bramham-Law, C.W.F., Smith, V.C., 2014. Cryptotephra as
496 a dating and correlation tool in archaeology. Journal of Archaeological Science 42, 42-50.

497 Larsen, J.J., 2013. Lateglacial and Holocene tephrostratigraphy in Denmark Volcanic Ash in a
498 Palaeoenvironmental Context. Unpublished PhD Thesis. University of Copenhagen.

499 Larsen, J.J., Noe-Nygaard, N. 2014. Lateglacial and early Holocene tephrostratigraphy and
500 sedimentology of the Store Slotsenf basin, SW Denmark: a multi-proxy study. Boreas, 43,
501 349-361.

502 Lilja, C., Lind, E.M., Morén, B., Wastegård, S., 2013. A Lateglacial–early Holocene
503 tephrochronology for SW Sweden. Boreas 42, 544–554.

504 Lind, E.M., Wastegård, S., 2011. Tephra horizons contemporary with short early Holocene
505 climate fluctuations: new results from the Faroe Islands. *Quaternary International* 246, 157–
506 167.

507 Longman, J., Ersek, V., Veres, D., Salzmann, U., 2017a. Detrital events and hydroclimate
508 variability in the Romanian Carpathians during the Mid-to-Late Holocene. *Quaternary*
509 *Science Reviews* 167, 78–95.

510 Longman, J., Veres, D., Ersek, V., Salzmann, U., Hubay, K., Bormann, M., Wennrich, V., and
511 Schäbitz, F., 2017b. Periodic input of dust over the Eastern Carpathians during the Holocene
512 linked with Saharan desertification and human impact. *Climate of the Past* 13, 897-917.

513 Lowe, J.J., Ramsey, C.B., Housley, R. A., Lane, C.S. and Tomlinson, E.L., 2015. The RESET
514 project: constructing a European tephra lattice for refined synchronisation of environmental
515 and archaeological events during the last c. 100 ka. Vedde Ash layer discovered in a small
516 lake basin on the Scottish mainland 118, 1–17.

517 Lowe, J.J., Palmer, A.P., Carter-Champion, A., MacLeod, A., Ramirez-Rojas, I., Timms, R.G.O.,
518 2017. Stratigraphy of a Lateglacial lake basin sediment sequence at Turret Bank, upper Glen
519 Roy, Lochaber: implications for the age of the Turret Fan. *Proceeding of the Geologists’*
520 *Association*. 128, 110-124.

521 Maclead, A., Brunnberg, L., Wastegård, S., Hand, T., Matthews, I.P., 2014. Lateglacial
522 cryptotephra detected within clay varves in Östergötland, south-east Sweden. *Journal of*
523 *Quaternary Science* 29: 605–609.

524 Magyari, E.K., Braun, M., Buczkó, K. Kern, Z., László, P., Hubay, K., 2009. Radiocarbon
525 chronology of glacial lake sediments in the Retezat Mts (South Carpathians, Romania): A

526 window to Late Glacial and Holocene climatic and palaeoenvironmental changes. Central
527 European Geology 52: 225–248.

528 Magyari, E.K., Jakab, G., Bálint, M., Kern, Z., Buczkó, K., Braun, M., 2012. Rapid vegetation
529 response to Lateglacial and early Holocene climatic fluctuation in the South Carpathian
530 Mountains (Romania). Quaternary Science Reviews 35, 116–130.

531 Moreno, A., Svensson, A., Brooks, S.J., Connor, S., Engels, S., Fletcher, W., Genty, D., Heiri,
532 O., Labuhn, I., Perşoiu, A., Peyron, O., Sadori, L., Valero-Garcés, B., Wulf, S. and Zanchetta,
533 G., 2014. A compilation of Western European terrestrial records 60–8 ka BP: towards an
534 understanding of latitudinal climatic gradients. Quaternary Science Reviews 106, 167–185.

535 Newhall, C.G., Self, S., 1982. The volcanic explosivity index (VEI) an estimate of explosive
536 magnitude for historical volcanism. Journal of Geophysical Research 87, 1231-1238.

537 Norddahl H., Hjort C., 1993. Lateglacial raised beaches and glacier recession in the
538 Pistilfjörður-Bakkaflói area, Northeast Iceland. Jökull 43, 33–44.

539 Orbán, I., Birks H.H., Vincze, I., Finsinger, W., Pál, I., Marinova, E., Jakab, G., Braun, M.,
540 Hubay, K., Bíró, T., Magyari, E.K., 2017. Treeline and timber- line dynamics on the northern
541 and southern slopes of the Retezat Mountains (Romania) during the Late-Glacial and the
542 Holocene. Quaternary International in press, DOI: 10.1016/j. quaint.2017.03.012.

543 Ott, F., Wulf, S., Serb, J., Słowinski, M., Obremska, M., Tjallingii, R., Błaszczewicz, M., Brauer,
544 A., 2016. Constraining the time span between the Early Holocene Hasseldalen and Askja-S
545 Tephra through varve counting in the Lake Czechowskie sediment record, Poland. Journal
546 of Quaternary Science 31, 103– 113.

547 Pál, I., Magyari, E.K., Braun, M., Vincze, I., Pálffy, J., Molnár, M., Finsinger, W., Buczko, K.,
 548 2016. Small-scale moisture availability increase during the 8.2-ka climatic event inferred
 549 from biotic proxy records in the South Carpathians (SE Romania). *The Holocene* 26:9, 1382-
 550 1396.

551 Pál I., Buczkó, K., Vincze, I., Finsinger, W., Braun, M., Biró, T., Magyari, E., in press. Terrestrial
 552 and aquatic ecosystem responses to early Holocene rapid climate change (RCC) events in
 553 the South Carpathian Mountains, Romania. *Quaternary International*
 554 <https://doi.org/10.1016/j.quaint.2016.11.015>

555 Pilcher, J., Bradley, R.S., Francus, P., Anderson, L., 2005. A Holocene tephra record from the
 556 Lofoten Islands, arctic Norway. *Boreas* 34, 136–156.

557 Pyne-O'Donnell, S., 2011. The taphonomy of Last Glacial-Interglacial Transition (LGIT) distal
 558 volcanic ash in small Scottish lakes. *Boreas* 40, 131–145.

559 Raner, P.H., Allen, J.R., Huntley, B., 2005. A new early Holocene cryptotephra from
 560 northwest Scotland. *Journal of Quaternary Science* 20:3, 201-208.

561 Reimer, P.J., Bard, E., Bayliss, A., Beck, J.W., Blackwell, P.G., Bronk Ramsey, C., Buck, C.E.,
 562 Cheng, H., Edwards, L.R., Friedrich, M., Grootes, P.M., Guilderson, T.P.,
 563 Hafliðason, H., Hajdas, I., Hatte, C., Heaton, T.J., Hoffmann, D.L., Hogg, A.G., Hughen, K.A.,
 564 Kaiser, K.F., Kromer, B., Manning, S.W., Niu, M., Reimer, R.W., Richards, D.A., Scott, E.M.,
 565 Southon, J.R., Staff, R.A., Turney, C.S.M., van der Plicht, J., 2013. IntCal13 and Marine13
 566 radiocarbon age calibration curves 0- 50,000 years cal BP. *Radiocarbon* 55, 1869-1887.

567 Sigvaldason, G.E., 2002. Volcanic and tectonic processes coinciding with glaciation and
 568 crustal rebound: an early Holocene rhyolitic eruption in the Dyngjufjöll volcanic centre and

569 the formation of the Askja caldera, north Iceland. *Bulletin of Volcanology* 64:192-205.

570 Sæmundsson, K., 1991. The geology of the Krafla system (Jarðfræði Kröflukerfisins). In:

571 Garðarsson, A., Einarsson, A. (Eds). *Náttúra Mý vatns*. Hið íslenska náttúrufræðifélag,

572 Reykjavík, pp 25–95.

573 Steffensen, J.P., Andersen, K.K., Bigler, M., Clausen, H.B., Dahl-Jensen, D., Fischer, H.,

574 Gotoazuma, K., Hansson, M., Johnsen, S.J., Jouzel, J., Masson-delmotte, V., Popp, T.,

575 Rasmussen, S.O., Röthlisberger, R., Ruth, U., Stauffer, B., Sveinbjörnsdóttir, Á.E., Svensson,

576 A. and White, J.W.C., 2008. High-Resolution Greenland Ice Core Data Show Abrupt Climate

577 Change Happens in Few Years. *Science* 321:5889, 680-684.

578 Striberger, J., Björck, S., Holmgren, S., Hamerlík, L., 2012. The sediments of Lake Lögurinn—a

579 unique proxy record of Holocene glacial meltwater variability in eastern Iceland. *Quaternary*

580 *Science Reviews* 38, 76–88.

581 Timms, R.G.O., Matthews, I.P., Palmer, A.P., Candy, I., Abel, L., 2016. A high-resolution

582 tephrostratigraphy from Quoyloo Meadow, Orkney, Scotland: implications for the

583 tephrostratigraphy of NW Europe during the Last Glacial-Interglacial Transition. *Quaternary*

584 *Geochronology*

585 Tomlinson, E.L., Arienzo, I., Civetta, L., Wulf, S., Smith, V.C., Hardiman, M., Lane, C.S.,

586 Carandenta, A., Orsi, G., Rosi, M., Muller, W., Menzies, M.A., 2012. Geochemistry of the

587 Phlegraean Fields (Italy) proximal sources for major Mediterranean tephras: Implications for

588 the dispersal of Plinian and co-ignimbritic components of explosive eruptions. *Geochimica*

589 *et Cosmochimica Acta* 93, 102-128.

590 Tomlinson, E.L., Smith, V.C., Albert, P.G., Aydar, E., Civetta, L., Cioni, R., Çubukçu, E.,
 591 Gertisser, R., Isaia, R., Menzies, M.A., Orsi, G., Rosi, M., Zanchetta, G., 2015. The major and
 592 trace element glass composition of the productive Mediterranean volcanic sources: tools for
 593 correlating distal tephra layers in and around Europe. *Quaternary Science Reviews* 118, 48-
 594 66.

595 Tóth, M., Magyari, K., Brooks, S.J., Braun, M., Buczkó, K., Bálint, M., Heiri, O., 2015. A
 596 chironomid-based reconstruction of late glacial summer temperatures in the southern
 597 Carpathians (Romania). *Quaternary Research* 77, 122–131.

598 Tóth, M., Buczkó, K., Specziár, A., Heiri, O., Braun, M., Hubay, K., Czakó, D., Magyari, E., in
 599 press. Limnological changes in South Carpathian glacier-formed lakes (Retezat Mountains,
 600 Romania) during the Late Glacial and the Holocene: A synthesis. *Quaternary International*, in
 601 press, <https://doi.org/10.1016/j.quaint.2017.05.023>

602 Turney, C. S. M., Harkness, D. D., Lowe, J. J. 1997. The use of microtephra horizons to
 603 correlate late-glacial lake sediment successions in Scotland. *Journal of Quaternary Science*
 604 12:6, 525-531.

605 Turney, C.S.M., 1998. Extraction of rhyolitic component of Vedde microtephra from
 606 minerogenic lake sediments. *Journal of Paleolimnology* 19, 199-206.

607 Turney, C.S.M., Van Den Burg, K., Wastegård, S., Davies, S.M., Whitehouse, N.J., Pilcher,
 608 J.R., Callaghan, C., 2006. North European last glacial-interglacial transition (LGIT; 15-9 ka)
 609 tephrochronology: extended limits and new events. *Journal of Quaternary Science* 21, 335–
 610 345.

611 Veres, D., Lane, C.S., Timar-Gabor, A., Hambach, U., Constantin, D., Szakács, A., Fülling, A.,

612 Onac, B.P., 2013. The Campanian Ignimbrite/Y5 tephra layer – A regional stratigraphic
 613 marker for Isotope Stage 3 deposits in the Lower Danube region, Romania. *Quaternary*
 614 *International* 293, 22–33.

615 Vincze, I., Orbán, I., Birks, H.H., Pál, I., Finsinger, W., Hubay, K., Marinova, E., Jakab, G.,
 616 Braun, M., Biró, T., Tóth, M., Danau, C., Ferencz, I.V., Magyari, E.K., 2017. Holocene treeline
 617 and timberline changes in the South Carpathians (Romania): climatic and anthropogenic
 618 drivers on the southern slopes of the Retezat Mountains. *Holocene*, in
 619 press, <https://doi.org/10.1177/0959683617702227>.

620 Wastegård, S., Björch, S., Possner, G., Wohlfarth, B., 1998. Evidence for the occurrence of
 621 Vedde Ash in Sweden: radiocarbon and calendar age estimates. *Journal of Quaternary*
 622 *Science* 13:3, 271-274.

623 Wastegård, S., Wohlfarth, B., Subetto, D.A., Sapelko, T.V., 2000. Extending the known
 624 distribution of the Younger Dryas Vedde Ash into northwestern Russia. *Journal of*
 625 *Quaternary Science* 15:6, 581-586.

626 Watson, E.J., Swindles, G.T., Lawson, I.T., Savov, I.P., Wastegård, S., 2017. The presence of
 627 Holocene cryptotephra in Wales and southern England. *Journal of Quaternary Science* 32,
 628 493–500.

629 Wohlfarth, B., Blaauw, M., Davies, S.M., Andersson, M., Wastegård, S., Hormes, A., Possner,
 630 G., 2006. Constraining the age of Lateglacial and early Holocene pollen zones and tephra
 631 horizons in southern Sweden with Bayesian probability methods. *Journal of Quaternary*
 632 *Science* 21: 321–334.

633 Wulf, S., Dräger, N., Ott, F., Serb, J., Appelt, O., Guðmundsdóttir, E., van den Bogaard, C.,
634 Słowinski, M., Błaskiewicz, M., Brauer, A., 2016b. Holocene tephrostratigraphy of varved
635 sediment records from Lakes Tiefer See (NE Germany) and Czechowskie (N Poland).
636 Quaternary Science Reviews 132, 1–14.

